of the Nigerian Association of Mathematical Physics
Volume **22 (November, 2012), pp 73 – 84**

Radiative Forcing of Saharan Aerosols in the Near Infrared Regions

B. I. Tijjani
Department of Physics, Bayero University, Kano

Abstract

We study the radiative forcing of Saharan aerosols at the near infrared region $(1.0\,\mu m\ to\ 4.0\,\mu m)$ ***using data from the Optical Properties of Aerosol and Clouds software . Radiative forcing at different wavelengths and Relative humidities are calculated and analysed. We also analysed the effective refractive indicies, optical depths, single scattering albedo, and extinction, scattering and absorption coefficients able to enable us to understand the nature of the particles and their size distributions. From the analysis, it was discovered that radiative forcing (in a form of cooling) increases with the increase in relative humidities (RH) and is dependent on wavelengths and the types of particle size distributions. The value of Angstrom constant at 0% RH reflects the dominance of large particles. But as the RH increases the parameter continues to increase indicating the increase in the concentrations of smaller particles due to the sedimentation of larger particles. This is because as the RH increases, large particles continue to sediment which results in the increase in the concentrations of smaller particles that causes decrease in effective radii which results in the increase in Angstrom constant and increase in radiative cooling. The analysis of the Angstrom coefficients and the nature of the increase in radiative cooling showed the dominance of large particles. The analysis of optical depth with wavelengths together with the comparison with scattering and absorption coefficients, hygsroscopicity factor and humidification factor it is discovered that the particles have bimodal type of size distributions with majority satisfying Junge type of distribution with a small component of larger particles satisfying lognormal.***

1.0 Introduction

The Sahara is a major source of dust aerosols [1] and the dust transport from the Sahara is an important climatic process [2-5]. The aerosols reflect the incoming solar radiation to space, thereby reducing the amount of sunlight available to the ground. This is called the 'direct' radiative effect of aerosols. The aerosols also serve as cloud condensation nuclei and change the cloud albedo and microphysical properties of clouds, which is called the 'indirect' radiative effect. The effect of aerosols is comparable in magnitude but opposite in sign to that of the greenhouse effect [6]. While the effect of aerosols is to reduce the surface temperature, the increase in greenhouse gases increases the surface temperature [3]. The magnitude of the global mean radiative forcing of dust aerosols is comparable to that of anthropogenic aerosols from sulphate and biomass combustion [7,8]. There are considerable uncertainties in estimating the radiative effects of dust aerosols. The net radiative forcing at the top-of-atmosphere (TOA) could be either positive or negative, depending on several key variables such as surface albedo, particle size, vertical distribution of the dust layer, dust optical depth (τ), and the imaginary part of the refractive index [2,9]. The optical depth is a very valuable aerosol characteristic, which is a key parameter for various aerosol related studies such as aerosol radiative forcing, atmospheric corrections on aerosol effect on remote sensing, etc. [10].
Current understanding of the radiative forcing of dust aerosols is very limited [11], especially over dust source regions where ground observations are few and multispectral satellite retrievals at visible to near-infrared wavelengths are often difficult due to the high surface albedo [12]. The ultraviolet, visible, near-infrared and infrared spectral regions are increasingly being

Corresponding author-, E-mail: idrith@yahoo.com, idrihtijjani@gmail.com, Tel. +234 8037030877

exploited for the remote sounding of the Earth's atmosphere and surface [13]. Aerosol optical properties are dependent on size distribution, shape, chemical composition, and mixing state, all of which are strong functions of relative humidity (RH) [14]. Water uptake affects aerosol atmospheric lifetime and composition, which in turn affect atmospheric visibility, direct radiative forcing of climate (Intergovernmental Panel on Climate Change [15] and cloud microphysics [16]. Many studies have reported the humidity response of both laboratory-generated and atmospheric aerosols [17-19] and empirically derived f(RH, λ) are now incorporated into most chemical transport and radiative transfer models.

The aim of this paper is to calculate and analyze the spectral variation of Radiative forcing with relative humidities (0, 50, 70, 80, 90, 95, 98 and 99%) for saharan aerosols at the near-infrared region from the data extracted from OPAC. The spectral variations of optical depths, absorption, scattering and extinction coefficients are analysed to determine the particles size distributions and the effect of hygroscopic growth as a result of increase in RH with the change in mode size distributions.

2.0 Methodology

The data used for the Saharan dust in this paper are derived from the Optical Properties of Aerosols and Clouds (OPAC) data set [20]. In this, a mixture of four components is used to describe desert aerosols: a water soluble components (WASO), and three mineral components of different sizes – mineral nucleation mode (MINM), mineral accumulation mode(MIAM) and mineral coarse mode (MICM).

The globally averaged direct aerosol Radiative forcing, ΔF_R, was calculated using the equation derived by [21],

$$\Delta F_R = -\frac{S_0}{4} T_{atm}^2 (1-N)\{(1-A)^2 2\beta\tau_{sca} - 4A\tau_{abs}\} \quad (1)$$

Where S_0 is a solar constant, T_{atm} is the transmittance of the atmosphere above the aerosol layer, N is the fraction of the sky covered by clouds, A is the albedo of underlying surface, β is the fraction of radiation scattered by aerosol into the atmosphere and τ_{sca} and τ_{abs} are the aerosol layer scattering and absorption optical thicknesses respectively. The above expression gives the radiative forcing due to the change of reflectance of the earth-aerosol system. The upscattering fraction is calculated using an approximate relation [22]

$$\beta = \frac{(1-g/2)}{2} \quad (2)$$

The global averaged albedo A=0.22 over land and A=0.06 over the ocean with 80% of aerosols being over the land; solar constant of 1370Wm^{-2}, the atmospheric transmittance is taken to be T_{atm}=0.79 [23] and cloudness N=0.6.

To determine the relationship between wavelengths and effective refractive indices the following formula is used for the four mixed aerosols [24]:

$$\frac{\varepsilon_{eff}-\varepsilon_0}{\varepsilon_{eff}+2\varepsilon_0} = \sum_{i=1}^{4} f_i \frac{\varepsilon_i-\varepsilon_0}{\varepsilon_i+2\varepsilon_0} \quad (3)$$

Where f_i and ε_i are the volume fraction and dielectric constant of the i^{th} component ε_0 is the dielectric constant of the host material and ε_{eff} is the effective dielectric constant. For the case of Lorentz-Lorentz [25,26], the host material is taken to be vacuum, ε_0 =1.

A relationship between the size of atmospheric aerosol particles and the wavelength dependence of the extinction coefficient was first suggested by [27]. Since that time [27] empirical formula for the wavelength dependence of the extinction coefficient has been directly related to a parameter of a Junge size distribution [28-30] used the wavelength dependence of the particulate extinction coefficient in the visible and near-infrared regions to infer the aerosol size distributions existing above water in the Chesapeake Bay area. He determined that the majority of aerosol size distributions could best be represented by a two-component size distribution consisting of a Junge-type distribution plus a small component of larger particles. To use α as an index to model the variation of aerosol size distributions, a relationship between α and the size distribution must be established. Several studies have shown that α is closely related to the aerosol size distributions [31,32]. By assuming that aerosols have a Junge distribution [33],

$$\frac{dN}{dln(r)} = r^n \quad (4)$$

It has been shown that α = n-2 [34]. However, the relationship between α and the size distribution may vary if aerosol size distribution does not follow a Junge size distribution [31]. The spectral behavior of the aerosol optical thickness, scattering, absorption, and extinction coeffecients can be used to obtain some information regarding the size distribution by just looking at the Angstron coefficient exponent that expresses the spectral dependence of aerosol optical depth (τ), scattering (σ_{scat}), absorption (σ_{abs}) and extinction (σ_{ext}) coefficients, with the wavelength of light (λ) as inverse power law [35]:

$$X(\lambda)=\beta\lambda^{-\alpha} \quad (5)$$

where X(λ) can be any of the parameters mentioned above. In this paper optical depths (τ(λ))are used but the other parameters are used for comparisons. The formula is derived on the premise that the extinction of solar radiation by aerosols is a continuous function of wavelength, without selective bands or lines for scattering or absorption [36]. The wavelength dependence of τ(λ) can be characterized by the Angstron parameter, which is a coefficient of the following regression:

$$\ln\tau(\lambda) = -\alpha\ln(\lambda) + \ln\beta \quad (6)$$

where β and α are the turbidity coefficient and the shaping factor, respectively [34,37], they are determined using SPSS 15 for windows.. The shaping factor α is related to the size of particles and provides a measure of how rapidly aerosol optical depth τ changes with wavelength. The value of α depends on the ratio of the concentration of large to small aerosols and β represents the total aerosol loading in the atmosphere. So α and β can be used to describe the size distribution of aerosol particles and the general haziness of the atmosphere. Larger particles generally correspond to smaller α, whereas smaller particles generally correspond to larger α. According to [38] a low, (down to 0) is a sign of large dust particles; a high (up to 2) corresponds to small smoke particles. According to [39], typical values of the shaping factor are larger than 2.0 for fresh smoke particles and close to zero for Sahelian Saharan dust particles. The dust studies seem to yield shaping factors in the range of approximately 0.2, whereas particles produced from biomass burnings yielded shaping factors around 1.5 and higher. For Saharan dust, the classical Angström coefficient α, is very small and can be even slightly negative over some wavelength interval and fluctuations of α, reflect variations in the size spectrum. [40,41]. The Ångström exponent values are high for shorter wavelengths and low in longer wavelengths. Large positive values of α are characteristic of fine-mode-dominated aerosol size distributions [36,42,43] while near zero and negative values are characteristic of dominant coarse-mode or bi-modal size distributions, with coarse-mode aerosols having significant magnitude [42,44,45]. When the particle size distribution is dominated by small particles, a situation usually associated with pollution, the Ångström coefficients are high; in clear conditions they are usually low. [46] demonstrated that the Ångström coefficient can be used as a tracer of continental aerosols. With changing atmospheric conditions and rising or falling RH, the measured aerosol optical thickness/extinction likewise changes, and so does the Ångström coefficient. In the analysis of spectral measurement of optical thickness in locations dominated by biomass burning, urban, or desert dust aerosols, a significant curvature in the ln τ versus ln λ relationship was observed [42]. In this paper an attempt has been made to show that, for some spectral range, departure from power law behavior from τ is observed, which is dependent on the aerosol type. This departure introduces a curvature on lnτ versus lnλ curve. And a second order fit to the lnτ versus lnλ provides better estimates than linear fit [43,45,47]. The quadratic formula that is used is

$$\ln\tau = -\alpha_2(\ln\lambda)^2 - \alpha_1\ln\lambda + \ln\beta \qquad (7)$$

and the coefficients (β, α_1, α_2) are obtained. In case of negative curvature ($\alpha_2<0$, convex type curves) the rate of change of α is more significant at the longer wavelengths, while in case of positive curvature ($\alpha_2>0$, concave type curves) the rate of change of α is more significant at the shorter wavelengths. [42] reported the existence of negative curvatures for fine-mode aerosols and positive curvatures for significant contribution by coarse-mode particles in the size distribution. The initial use of α_2 of optical depth in equation (7) for classification of aerosols was determined by [42] and in some of his subsequent publications [43,48]. The application of this relationship is to give further insight into the properties of aerosols [49].

To quantify the water uptake at subsaturated conditions, we define the hygroscopic growth factor (HGF) as the ratio of the radius R_{RH}, at a specified RH to the original dry radius R_{dry}, which is at an RH=0% [50,51]:

$$HGF = \frac{R_{RH}}{R_{dry}} \qquad (8)$$

In this paper, HGF is calculated at 50, 70, 80, 90, 95, 98 and 99% RH. The HGF can be subdivided into different classes with respect hygroscopicity. One classification is based on diameter growth factor by [50,52] as Barely Hygroscopic (BH; HGF = 1.0–1.11), Less Hygroscopic (LH; HGF = 1.11–1.33), More Hygroscopic (MH; HGF = 1.33–1.85) .

In order to better describe the nature of particle in terms of estimate of direct climate forcing by aerosols and reduce the associated uncertainty, quantification of aerosol optical properties and their dependency on relative humidity [11,53,54] is important. The increase in light-scattering, absorption and extinction coefficients by aerosols with RH at a specific wavelength, f(RH, λ), (described as humidification factor), has been considered an important parameter for further description of aerosol Radiative forcing [11,55-61]. The hygroscopic growth of aerosols influences the particle size distribution and refractive indices and hence, several key optical properties of aerosols (e.g., scattering, extinction and absorption coefficients, single scattering albedo, asymmetry parameter, and aerosol optical depth) that are relevant to aerosol radiative forcing estimates [11,53,54].

The aerosol humidification factor, f(RH, λ), describes the ratio of aerosol light scattering between two different RH values. It was calculated from the following [17]:

$$f(RH,\lambda) = \frac{\sigma_{ext}(RH_{high},\lambda)}{\sigma_{ext}(RH_{high},\lambda)} = \left(\frac{100-RH_{ref}}{100-RH_{high}}\right)^{\gamma} \qquad (8)$$

where γ is referred to as the aerosol hygroscopicity factor. Hygroscopic properties of aerosol particles describe the interactions between particles and surrounding water vapor including the critical size needed to activate the growth of a particle into a cloud droplet by water vapor condensation in given conditions. The γ parameter in our case was obtained by combining the eight $\sigma_{ext}(\lambda)$ values at 00%, 50%, 70%, 80%, 90%, 95%, 98% and 99% RH. The use of γ has the advantage of describing the hygroscopic behavior of aerosols in a linear manner over a broad range of RH values; it also implies that particles are deliquesced [62]. The γ parameter is dimensionless, and it increases with increasing particle water uptake. From previous studies, typical values of γ for ambient aerosol ranged between 0.1 and 1.5 [62-64].

3.0 Results and Discussions

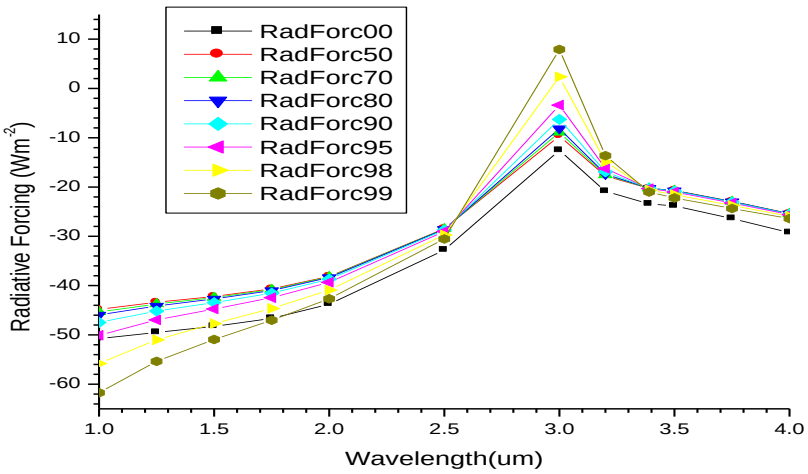

Figure 1: A graph of radiative forcing against wavelengths

The nature of the graphs at shorter wavelengths reflects the presence of fine particles, because fine particles usually scatter more light than coarse particles which results in greater cooling. Its relation with wavelengths shows the presence of having bimodal type of size distributions with the major one between 1.0μm and 2.5μm and small one at 2.5μm to 4.0μm. The behavior of the plots at the spectral of 1.0μm to 2.5μm shows the dominance of large particles with a very small concentration of small particles. The sign in the presence of small particles is because of the increase in radiative with the increase in RH, while at the interval 2.5μm to 4.0μm shows the complete absence of small particles because the radiative cooling is decreasing with the increase in RH.

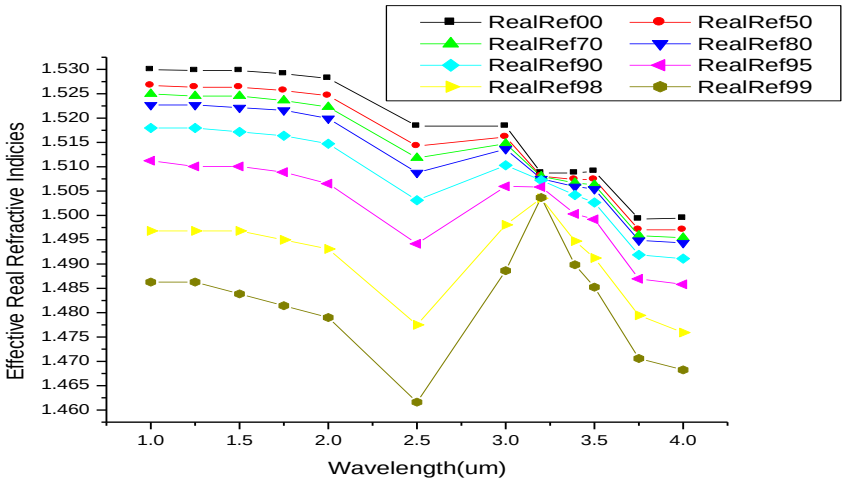

Figure 2: A graph of effective real refractive indices against wavelength

Figure 2 shows that effective real refractive indices decrease with the increase in RH which indicated the presence of fine mode particles. The decrease of indices with RH is as of the internal mixture of the aerosols with water, this is because the refractive index of water is smaller than the refractive indices of the aerosols that is why the effective refractive indices of the mixture are decreasing with the increase in RH by assuming that they have internal mixing. But its behavior with wavelength indicates the dominance of non-spherical particles because they are responsible for sensitivity of index with wavelengths [65].

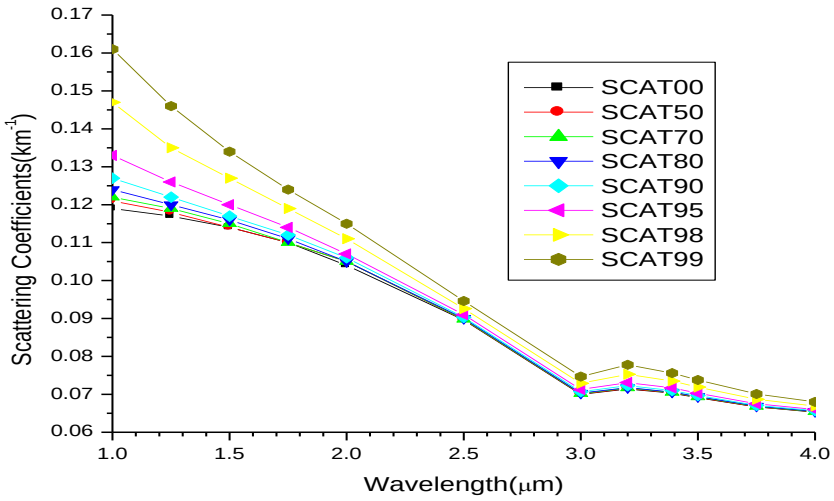

Figure 3: A plot of scattering coefficients against wavelength

From figure 3 bimodal type of size distribution in the form of Junge (1.0μm to 3.0μm) major component and a small lognormal (3.0μm to 4.0μm) can be observed. The nature of its relation with wavelengths and RH indicates the little presence of small particles because they scatter more light at shorter wavelengths and as a result of hygroscopic growth. It also shows that hygroscopic growth has caused increase in mode size distributions, which shows that particles size distributions are sensitive to both wavelengths and RHs. Though the studies by [66] said that the α (particle size distribution) value depends strongly on the spectral range used in its determination, but in our case we assume that different wavelengths are sensitive to different characteristics of the size distributions and RH.

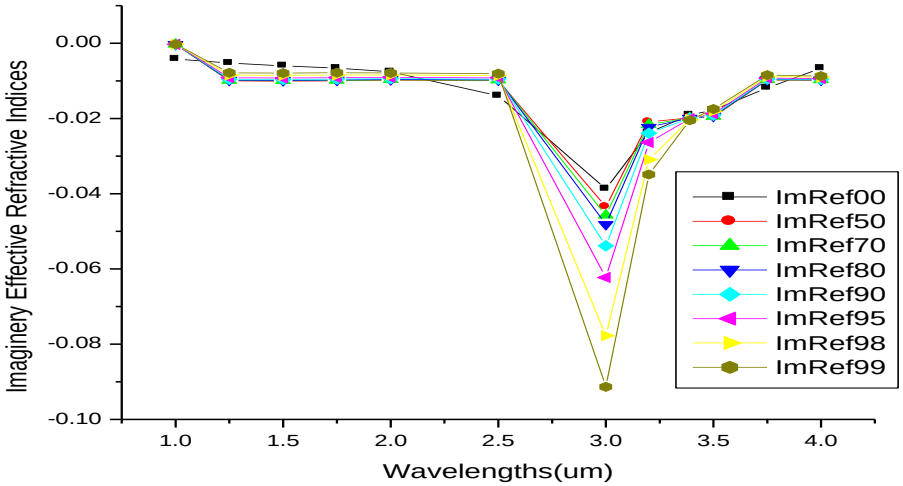

Figure 4: A plot of effective imaginary refractive indices against wavelengths

Figure 4 shows imaginary effective refractive indices is more sensitive to both wavelengths and RH at atmospheric window of 3.0μm which is the boundary between two types of distributions. It also shows the dominance of large particles because large particles have very small imaginery refractive indices.

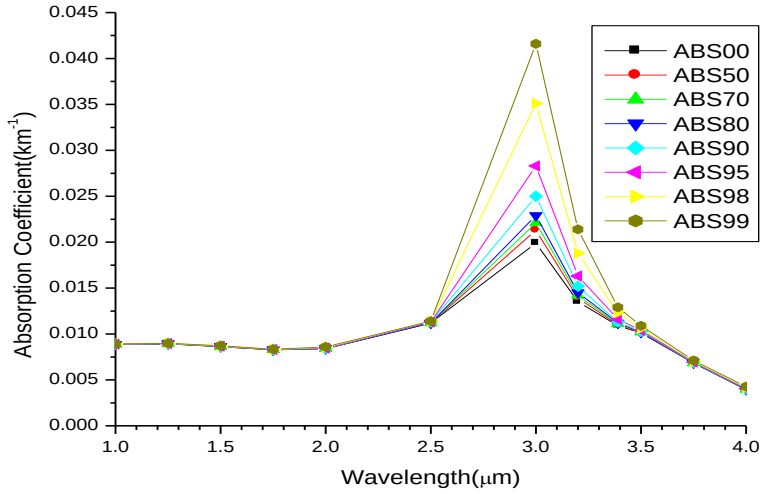

Figure 5: A graph of absorption against wavelengths.

It shows that the relation of absorption coefficient with wavelengths and RH is that it is more sensitive at the particle size change atmospheric window of 3.0μm. Its relation with wavelengths between 1.0 μm to 3.0 μm shows that it can satisfy Junge type size distribution with Angstrom exponents negative , which shows the dominance of coarse particles as cited by [42,44].

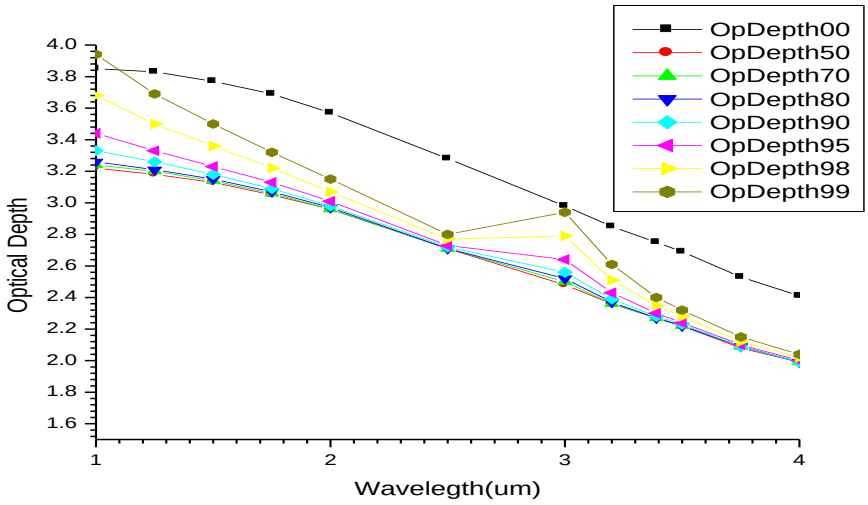

Figure 6: A graph of optical depth against wavelengths.

From figure 6 at 0% RH it looks as if there is only one mode of distribution of the form of Junge, and the nature of the dependence of optical depth with wavelengths indicates the dominance of large particles. But as the RH increases, bimodal type of distribution can be observed of the form of Junge type (1.0μm to 2.5μm) and lognormal (2.5μm to 4.0μm). But as a result of increase in RH to 50% it can be observed that there is a decrease in optical depth, which occurs as a result of condensation /sedimentation of large particles due to the increase in RH. But later the optical depths started to increase with RH as a result of the increase in the concentrations and contributions of smaller particles as a result of hygroscopic growth. This shows that increase in RH has created additional mode size distribution and also increase in mode size distributions.

Table 1: results of the Angstron coefficients at the respective relative humidities using equations (6) and (7) at the spectral range 1.0μm to 2.5μm.

	Linear			Quadratic			
RH	A	B	R^2	α_1	α_2	β	R^2
0	0.1652	3.9529	0.8297	-0.0680	0.2563	3.8368	0.9956
50	0.1784	3.2997	0.8574	-0.0480	0.2489	3.2055	0.9960
70	0.1848	3.3202	0.8697	-0.0375	0.2444	3.2271	0.9960
80	0.1923	3.3436	0.8825	-0.0255	0.2394	3.2518	0.9961
90	0.2109	3.4047	0.9096	0.0052	0.2262	3.3163	0.9965
95	0.2411	3.5095	0.9390	0.0518	0.2081	3.4256	0.9971
98	0.3044	3.7484	0.9701	0.1416	0.1789	3.6712	0.9979
99	0.3638	4.0035	0.9823	0.2168	0.1617	3.9289	0.9984

The observed variations in Ångström coefficients can be explained by changes in the effective radius of the mixture resulting from increase in RH: the larger the number of small aerosol particles, the smaller the effective radius and the larger the Ångström coefficient. This shows that hygroscopic growth has caused reduction in the effective radii because of sedimentation of large particles as a result of hygroscopic growth. Comparing the coefficients of determinations for both linear and quadratic, it can be observed that at 0% RH there is an improvement with $\alpha_2 > 0$, which shows the dominance of coarse particles in this region [42]. The decrease in values of α_2 as RH increases reflects the increase in the concentration of small particles, which tallies with the increase in α as the RH increases.

Though studies by [66] showed that the α value depends strongly on the spectral range used in its determination but in this study we discovered that it also depends on particles' sizes and RH. The increase in optical depths with the increase in RH is linked to a hygroscopic and/or coagulation growth from the fine aerosols. Furthermore, the fine mode aerosols have hydrate and coagulated characters that made them to become large particles, causing the optical depths to increase. The Ångström exponent increases with the increase in RH, which shows that large particles are sedimenting leaving smaller particles (that is increasing the number of smaller particles). A higher RH could obviously cause the particles' hygroscopic increase, which could result in greater extinction and a larger volume of fine particles.

Table 2: Data obtained from the microphysical properties using equation(7) for the Saharan aerosols.

RH(%)	0	50	70	80	90	95	98	99
HGF	1	1.002	1.003	1.004	1.006	1.008	1.0111	1.014
WASO(Vol. Mix %)	1.71	3.186	4.06	4.98	7.16	10.4	16.5	21.8

Table 2 is obtained using equation (8). It can be concluded that this mixture is barely hygroscopic (BH). This is not surprising because the percentage of WASO which is the part responsible for water absorption component is very small. The radii of hygroscopic aerosols grow up by uptake of water in humid air.

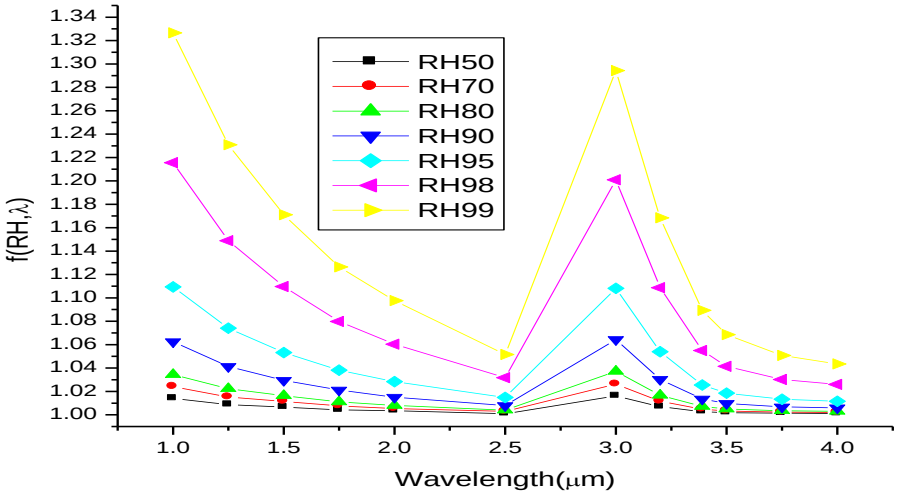

Figure 7: A graph of f(RH, λ) against wavelengths

This shows that the rate of increase of extinction with the increase in RH is very small, and this reflects the dominance of coarse particles. It also shows bimodal size distribution (ie Junge and lognormal). This shows that higher RH has caused the particles' hygroscopic increase. The relation of f(RH, λ) with RH is such that at the deliquescence point (90 to 99%) this growth with higher humidities increases substantially, making this process strongly nonlinear with relative humidity [67,68]. The low value of f(RH, λ) seem s to be related to low Angstrom exponent for Saharan dust. It also shows that f(RH, λ) is sensitive to different particles size distributions and increase in mode growth.

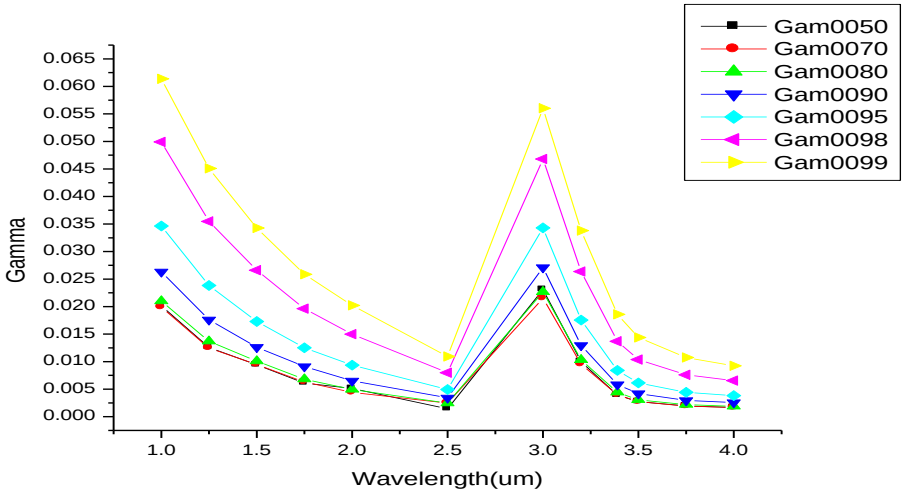

Figure 8: A graph of Gamma against wavelengths

The graph shows that the hygroscopicity of Saharan aerosols is very small. This is not surprising because they are dominated by coarse particles that are non-hygroscopic. It shows that it is very sensitive to particle size distributions and hygroscopic growth and shows bimodal size distribution (ie Junge and lognormal). It also shows that these particles are slightly deliquesced [62].

5.0 Conclusion

The radiative forcing (cooling) at 0%RH is about -50Wm^{-2} at 1.0μm, but at 50% it reduced to around -45Wm^{-2} and as the RH increases the cooling started increasing up to a maximum value of about -60Wm^{-2} at 99%. The nature of the increments of the radiative forcing with RH reflects the dominance of large particles. This is because as a result of increase in RH from 0 to 50%, large particles started sedimenting. But as the RH increases the concentrations of larger particles decrease and concentration of smaller particles continue to increase which result in decrease in effective radius and increase in Angstrom coefficients. The analysis of the Angstrom coefficients showed the dominance of large particles. The analysis of optical depth with wavelengths together with the comparison with scattering and absorption coefficients, hygsroscopicity factor and humidification factor show that the particles have bimodal type of size distributions with majority satisfying Junge type of distribution with a small component of lognormal.

Reference

[1] Prospero, J. M., (1990), Mineral–aerosol transport to the North Atlantic Ocean and North Pacific: the impact of Africa and Asian sources. In The long-range atmospheric transport of natural and contaminant substances, edited by A. H. Knap (Norwell, MA: Kluwer Academic), pp. 59–86.

[2] Tegen, I., and Lacis, A. A., (1996), Modeling of particle size distribution and its influence on the radiative properties of mineral dust aerosol. Journal of Geophysical Research, 101, 19237–19244.

[3] Hansen, J., Sato, M., Lacis, A., and Ruedy, R., (1997), The missing climate forcing. Transactions of the Royal Society of London, 352, 231–240.

[4] CoakleyJR J. A. and Cess, R. D., (1985), Response of the NCAR community climate model to the radiative forcing by the naturally occurring tropospheric aerosols. Journal of Atmospheric Science, 42, 1677–1692.

[5] Moulin, C., Dulac, F., Lambert, C. E., Chazette, P., Jankowiak, I., Chatenet, B., and Lavenu, F., (1997), Long-term daily monitoring of Sahara dust load over ocean using Meteosat ISCCP-B2 data: 2 accuracy of the method and validation using sun photometer measurements. Journal of Geophysical Research, 102, 16959–16969.

[6] IPCC (1995),Climate change. InTheScience of Climate Change, edited by J. T. Houghton, L. G. Meira Filho, J. Bruce, H. Lee, Callendar B. A., E. Haites, N. Harris and K.Maskell (New York: Cambridge University Press), pp. 69–124.

[7] IPCC (1994), Radiative forcing of climate change. In Climate Change 1994, edited by J. T. Houghton, L. G. Meira Filho, J. Bruce, H. Lee, B. A. Callendar, E. Haites, N. Harris and K. Maskell (New York: Cambridge University Press), pp. 131–157.

[8] Sokolik, I. N., and Toon, O. B., (1996), Direct radiative forcing by anthropogenic mineral aerosols. Nature, 381, 681–683.

[9] Liao, H., and Seinfeld, J. H., (1998), Radiative forcing by mineral dust aerosols: sensitivity to key variables. Journal of Geophysical Research, 103, 31637–31645.

[10] Kaufman, Y. J., Tanré D., Gordon H. R., Nakajima T., Lenoble J., Frouin R., Grassl H., Herman B. M., King M. D., and Teillet P. M.(1997) Passive remote sensing of tropospheric aerosol and atmospheric correction for the aerosol effect, *J. Geophys. Res*., *102*, 16,815-16,830,.

[11] IPCC, (2001): Climate Change 2001: The Scientific Basis. Houghton et al., Eds., Cambridge University Press, New York. 896 pp.

[12] Kaufman, Y. J., Tanre, D. and Boucher, O. (2002). A satellite view of aerosols in climate systems. Nature 419, 215–223.

[13] Buchwitz M., Rozanov V. V. and Burrows J. P. (2000) A correlated-k distribution scheme for overlapping gasses suitable for retrieval of atmospheric constituents from moderate resolution radiance measurements in the visible/near-infrared spectral region, ;Journal of Geophysical Research Vol.105, No. D12, p15247-15261

[14] Pilinis, C., Pandis S. N., and Seinfeld J. H. (1995), Sensitivity of direct climate forcing by atmospheric aerosols to aerosol size and composition, J. Geophys. Res., 100, 18,739 – 18,754.

[15] IPCC (2007), Climate Change 2007:Th e Physical Science Basis . Contribution of Working Group I to the Fourth Assessment Report of the Intergovernmental Panel on Climate Change, edited by S. Solomon et al., Cambridge Univ. Press, Cambridge, U. K.

[16] Lohmann, U., and J. Feichter (2005), Global indirect aerosol effects: A review, Atmos. Chem. Phys., 5, 715 – 737.

[17] Doherty, S. J., Quinn P. K., Jefferson A., Carrico C. M., Anderson T. L., and Hegg D. (2005), A comparison and summary of aerosol optical properties as observed in situ from aircraft, ship, and land during ACE-Asia, J. Geophys. Res., 11 0 , D04201, doi:10.1029/2004JD004964.

[18] Baynard, T., Garland R. M., Ravishankara A. R., Tolbert M. A., and Lovejoy E. R. (2006) , Key factors influencing the relative humidity dependence of aerosol light scattering, Geophys. Res. Lett. , 33 , L06813, doi:10.1029/2005GL024898.

[19] Garland, R. M., Ravishankara A. R., Lovejoy E. R., Tolbert M. A., and Baynard T. (2007), Parameterization for the relative humidity dependence of light extinction: Organic-ammonium sulfate aerosol, J. Geophys. Res.,11 2, D19303, doi:10.1029/2006JD008179.

[20] Hess, M., P. Koepke, and I. Schult, Optical properties of aerosols and clouds: The software package OPAC, *Bull. Amer. Meteor. Soc.*, *79*, 831-844, 1998.

[21] Chylek P. and Wong J. (1995), Effect of Absorbing aerosols of global radiation budget, Geophysical Research Letters, 22, 8, p929-931

[22] Segan, C. and Pollack J.(1967) Anisotropic nonconservative scattering and the clouds of Venus, J. Geophys. Res., 72, 469-477.

[23] Penner, J. E. Dickinson R.E. and O'Neil C. A. (1992) Effects of aerosols form biomass on the global radiation budget, Science, 256, 1432-1434.

[24] Aspens D. E. (1982), Local-field effect and effective medium theory: A microscopic perspective Am. J. Phys. 50, 704-709.

[25] Lorentz, H. A. (1880). Ueber die Beziehung zwischen der Fortpflanzungsgeschwindigkeit des Lichtes und der Korperdichte. Ann. P hys. Chem. 9, 641–665.

[26] Lorenz, L. (1880). Ueber die Refractionconstante. A nn. P hys. Chem. 11, 70–103.

[27] Angstrom, A., (1929): On the atmospheric transmission of sun radiation and on dust in the air. Geogr. Ann., 11, 156-166.

[28] van de Hulst, H. C., (1957): Scattering by Small Particles. Wiley, 470 pp.

[29] Junge, C. E (1963): Air Chemistry and Radioactisity. Academic Press, 382 pp.

[30] Curcio, J. A., (1961): Evaluation of atmospheric aerosol particle size distribution from scattering measurements in the visible and infrared. J. Opt. Sot. Arrw., 51, 548-551.

[31] Tomasi, C., E. Caroli, and V. Vitale, (1983)Study of the relationship between Angstrom's wavelength exponent and Junge particle size distribution exponent, J. Clim. Appl. Meteorol. , 22, 1707–1716.

[32] Reid, S. J., T. F. Eck, S. A. Christopher, P. V. Hobbs, and B. Holben, (1999) Use of Angstrom exponent to estimate the variability of optical and physical properties of aging smoke particles in Brazil, J. Geophys. Res., 104, 27, 473–27, 489.

[33] Junge, C. E.. (1955): The size distribution and aging of natural aerosols as determined from electrical and optical data on the atmosphere. J. Meteor.. 12, 13-25.

[34] Liou K. N.(2002) An Introduction to Atmospheric Radiation, 2nd ed. Academic, San Diego, Calif.,.

[35] Ångström, A.K. (1961). Techniques of Determining the Turbidity of the Atmosphere. Tellus XIII: 214.

[36] Ranjan, R.R., Joshi, H.P. and Iyer, K.N. (2007). Spectral Variation of Total Column Aerosol Optical Depth over Rajkot: A Tropical Semi-Arid Indian Station. Aerosol Air Qual. Res. 7: 33-45.

[37] O'Neill N. T., and Royer A. (1993) Extraction of binomial aerosol-size distribution radii from spectral and angular slope (Angstrom) coefficients, Appl. Opt. 32, 1642-1645.

[38] Dubovik, O., et. al., (2000): Accuracy assessments of aerosol optical properties retrieved from Aerosol Robotic Network (AERONET) Sun and sky radiance measurments, JGR, 105, 9791 - 9806.

[39] Eck T. F., Holben B. N., Reid J. S., Dubovik O., Smirnovm A., O'Neill N. T., Slutsker I., and Kinne S.,(2000) "An observational approach for determining aerosol surface radiative forcing: results from the first field phase of INDOEX," J. Geophys. Res. 105, 15347–15360.

[40] Prospero, J. M., Savoie D. L., Carlson T. N., and Ness R. T.(1979), Monitoring Saharan aerosol transport by means of atmospheric tubidity measurements, in Saharan Dust: Mobilisation, Transport, Deposition, Scope Rep. 14, edited by Morales C., John Wiley, New York.

[41] Carlson, T. N., and Caverly R. S. (1977) Radiative characteristics of Saharan dust at solar wavelengths, J. Geophys. Res., 87, 3141-3152.

[42] Eck, T.F., B.N.Holben, J.S.Reid, O.Dubovik, A.Smirnov, N.T.O'Neill, I.Slutsker, and S.Kinne, (1999) The wavelength dependence of the optical depth of biomass burning, urban and desert dust aerosols, *J.Geoph.Res., 104*, 31,333-31,350,.

[43] Eck, T. F., B. N. Holben, O. Dubovic, A. Smirnov, I. Slutsker, J. M. Lobert, and V. Ramanathan (2001), Column-Integrated aerosol optical properties over the Maldives during the northeast monsoon for 1998-2000 (2001), J. Geophys. Res., 106, D22, 28555-28566.

[44] O'Neill, N.T., Dubovic, O. and Eck, T.F. (2001). Modified Angstrom Exponent for the Characterization of Submicrometer Aerosols. Appl. Opt. 40: 2368-2375.

[45] Kaskaoutis, D.G. and Kambezidis, H.D. (2006). Investigation on Wavelength Dependence of the Aerosol Optical Depth in the Athens Area. Q.J.R Meteorol. Soc. 132: 2217-2234.

[46] Kusmierczyk-Michulec J. and A.M.J. van Eijk, (2007), Ångström coefficient as a tracer of the continental aerosols, Proceedings SPIE vol. 6708-25, Atmospheric Optics: Models, Measurements, and Target-in the-Loop Propagation, 27-28 August 2007, San Diego, CA, USA.

[47] Kaskaoutis, D. G., and H. D. Kambezidis, A. D. Adampoulos, and P. A. Kassomenos (2006), On the characterization of aerosols using the Ångström exponent in the Athens area, J. Atmos. Solar-Terr. Phys., 68, 2147-2163.

[48] Eck, T. F., et al. (2005), Columnar aerosol optical properties at AERONET sites i n cen tr al easte rn Asia a nd aer osol tr anspor t t o t he tropic al mid -Pacific, J. Geophys. Res. , 110 , D06202, doi:10.1029/2004JD005274

[49] Schuster, G.L., Dubovik, O. and Holben, B.N. (2006). Angstrom Exponent and Bimodla Aerosol Size Distributions. *J. Geophy. Res.* 111: 7207.

[50] Swietlicki, E.,et. al. (2008) Hygroscopic properties of submicrometer atmospheric aerosol particles mea-sured with H TDMA instruments in various environments – A review, Tellus B, 60, 432–469,.

[51] Randles , C. A. , Russell L. M. and. Ramaswamy V. (2004) Hygroscopic and optical properties of organic sea salt aerosol and consequences for climate forcing, GEOPHYSICAL RESEARCH LETTERS, VOL. 31, L16108, doi:10.1029/2004GL020628.

[52] Liu P. F., Zhao C. S., Gobel T., Hallbauer E., Nowak A., Ran L., Xu W. Y., Deng Z. Z., Ma N., Mildenberger K., Henning S., Stratmann F., and Wiedensohler A. (2011) Hygroscopic proper ties of aerosol par ticles at high relative humidity and their diurnal variations in the Nor th China Plain, Atmos. Chem. Phys. Discuss., 11, 2991–3040

[53] Penner, J.E., et al., (1994). Quantifying and minimizing uncertainty of climate forcing by anthropogenic aerosols. Bulletin of the American Meteorological Society 75, 375–400.

[54] Carrico, C.M., Kus, P., Rood, M.J., Quinn, P.K., Bates, T.S., (2003). Mixtures of pollution, dust, sea salt, and volcanic aerosol during ACE-Asia: radiative properties as a function of relative humidity. Journal of Geophysical Research 108 (D23), 8650.

[55] Charlson, R. J., Schwartz S. E., Hales J. M., Cess D., Coakley J. A., Hansen J. E., (1992) Climate forcing by anthropogenic aerosols. Science, 255, 423-430.

[56] Kotchenruther, R.A., Hobbs, P.V., Hegg, D.A., (1999). Humidi-fication factors for atmospheric aerosol off the mid-Atlantic coast of the United States. Journal of Geophysical Research 1043, 2239–2251.

[57] Im, J.-S., Saxena, V.K., Wenny, B.N., 2001. An assessment of hygroscopic growth factors for aerosols in the surface boundary layer for computing direct radiative forcing. Journal of Geophysical research 106 (D17), 20213–20224.

[58] Hegg, D.A., Covert, D.S., Crahan, K., (2002). The dependence of aerosol light scattering on RH over the Pacific Ocean. Geophysical Research Letters 29 (8), 1219.

[59] Magi, B.I., Hobbs, P.V., 2003. Effects of humidity on aerosols in Southern Africa during the biomass burning season. Journal of Geophysical Research 108 (D13), 8495.

[60] MaXling, A., Wiedensohler, A., Busch, B., NeusuX, C., Quinn, P., Bates, T., Covert, D., (2003). Hygroscopic properties of different aerosol types over the Atlantic and Indian Oceans. Atmospheric Chemistry and Physics 3, 1377–1397.

[61] Maria, S.F., Russell, L.M., Gilles, M.K., Myneni, S.C.B., (2004). Organic aerosol growth mechanisms and their climate-forcing implications. Science 306, 1921–1924.

[62] Quinn, P. K., Bates, T. S., Baynard, T., Clarke, A. D., Onasch, T. B., Wang, W., Rood, M. J., Andrews, E., Allan, J., Carrico, C. M., Coffman, D., and Worsnop, D.: Impact of particulate organic matter on the relative humidity dependence of light scattering: A simplified parameterization, Geophys. Res. Lett., 32, L22809, doi:10.1029/2005GL024322, 2005.

[63] Gasso, S., et al. (2000), Influence of humidity on the aerosol scattering coefficient and its effect on the upwelling radiance during ACE-2, Tellus, Ser. B , 52, 546 – 567.

[64] Clarke, A. McNaughton, C. Kapustin, V., Shinozuka, Y., Howell, S., Dibb, J., Zhou, J., Anderson, B., Brekhovskikh, V., Turner, H., and Pinkerton, M.(2007): Biomass burning and pollution aerosol over North America: organic components and their influence on spec-tral optical properties and humidification response, J. Geophys. Res., 112, D12S18, doi:10.1029/2006JD007777.

[65] Dubovik, O., Holben, B. N., Eck, T. F., Smirnov, A., Kaufman, Y. J., King, M. D., Tanre, D., and Slutsker, I.(2002): Climatology of atmospheric aerosol absorption and optical properties in key locations, J. Atmos. Sci., 59, 590–608.

[66] Cachorro, V.E., Vergaz R and de Frutos A.M. (2001). A Quantitative Comparison of α Angstrom Turbidity Parameter Retrieved in Different Spectral Ranges Based on Spectro-radiometer Solar Radiation Measurements, Atmos. Environ. 35: 5117-5124.

[67] Fitzgerald, J. W. (1975) Approximation formulas for the equilibrium size of an aerosol particle as a function of its dry size and composition and ambient relative humidity. J. Appl. Meteorol., 14, 1044 –1049

[68] Tang, I. N. (1996) Chemical and size effects of hygroscopic aerosols on light scattering coeffcients. J. Geophys . R es. , 101, 19245 – 19250